Supplemental Figures

Supplemental Figure 1

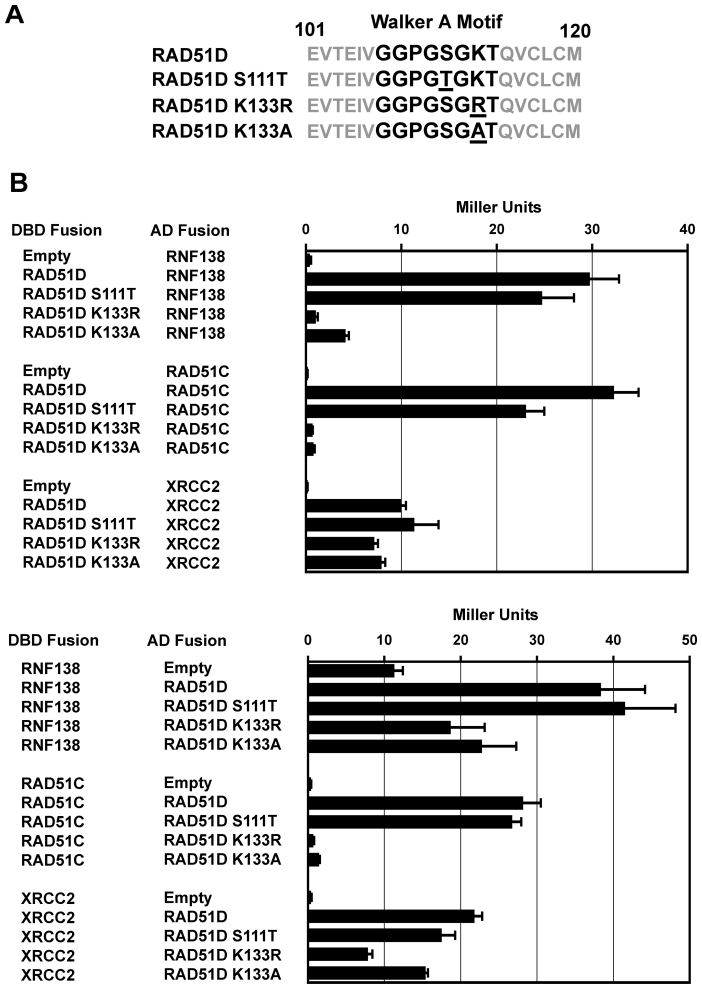

Fig. S1. RNF138 interaction with RAD51D requires the highly conserved RAD51D Walker A ATPase motif. (A) Amino acid residues substituted in the RAD51D Walker A Motif are underlined. (B) Y187 haploids were co-transformed with RNF138 and the indicated RAD51D WT or ATPase mutant plasmids. Protein interaction strengths were quantified by measuring β-galactosidase activity. Data represent mean +/- SEM from three independent experiments performed in triplicate. Abbreviations: *DBD Fusion*- GAL4 DNA binding domain fusion, *AD Fusion*- GAL4 activation domain fusion.

Supplemental Figure 2

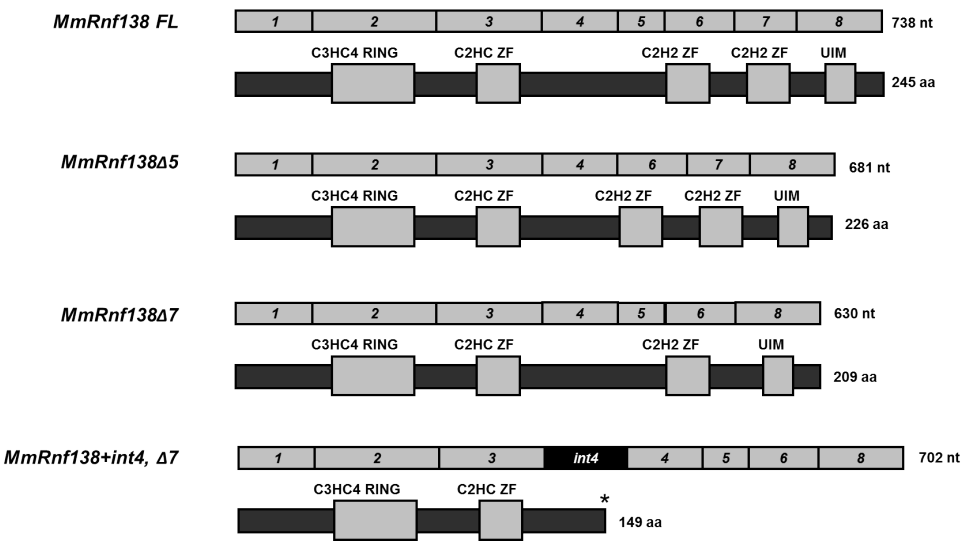

Fig. S2. Summary of *Mus musculus Rnf138* splice variants. The eight exons of *Rnf138* are displayed as numbered boxes drawn relative to base pair length. The full-length *Rnf138* mRNA transcript is shown along the top, and the alternatively spliced transcripts are displayed below. Predicted translation products are displayed beneath the transcripts. The black box represents the retained intron in *Rnf138+int4,Δ7*. The asterisk represents the premature termination codon. Open gray boxes mark sequence corresponding to the indicated functional domain. Abbreviations: *ZF-* zinc finger, *UIM-* ubiquitin interaction motif, *nt-* nucleotide, *aa-* amino acid.

Supplemental Figure 3

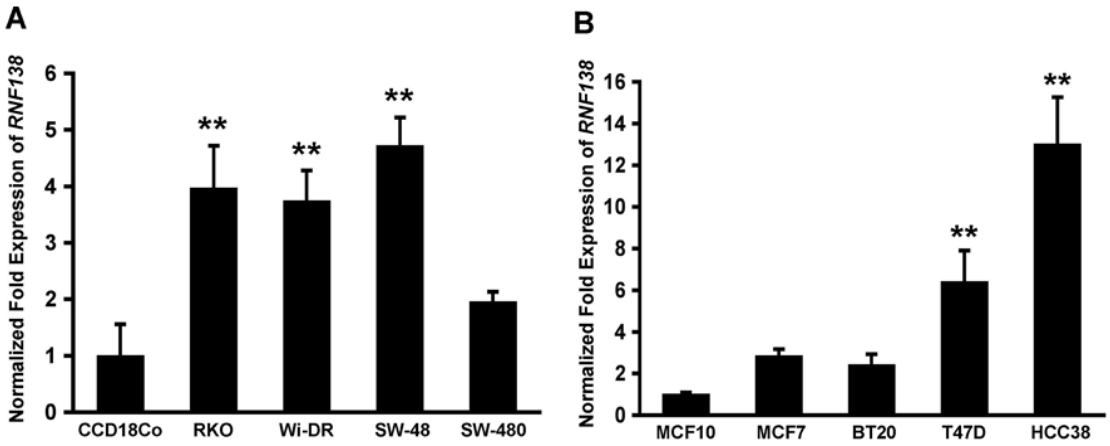

Fig. S3. Increased expression of *RNF138* in colon cancer and breast cancer cell lines. (A) Expression of *RNF138* in non-tumorigenic CCD18Co and four human colon cancer cell lines (RKO, Wi-DR, SW-48, and SW480). (B) Expression of *RNF138* in normal breast tissue (MCF10) and four human breast cancer cell lines (MCF7, BT20, T47D, and HCC38). Expression analysis was performed by quantitative real-time PCR, and all data was normalized to *GAPDH* mRNA levels. *RNF138* expression in each cancer cell line was compared to the non-tumorigenic sample to determine statistical significance. Error bars represent standard deviation from a representative experiment performed in triplicate and ** indicates $P < 0.01$.

Supplemental Figure 4

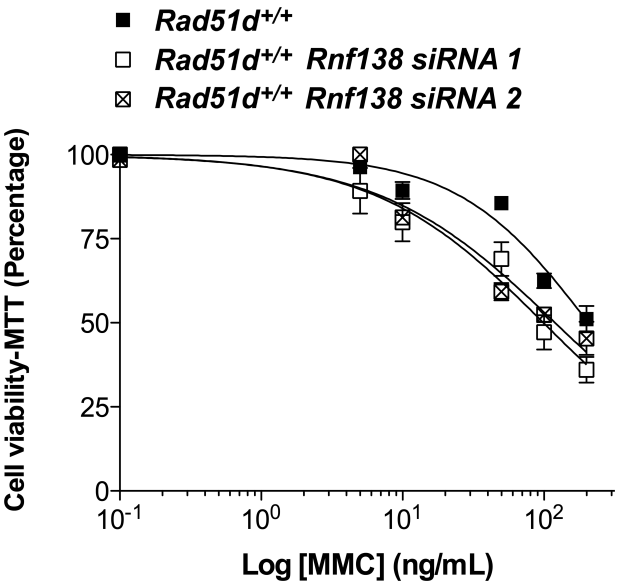

Fig. S4. RNF138 knockdown by an independent *Rnf138* siRNA duplex confers increased sensitivity to Mitomycin C. *Rad51d*$^{+/+}$ *(Rad51d*$^{+/+}$*, Trp53*$^{-/-}$*)* MEFs were transfected with *Rnf138* siRNA1 and *Rnf138* siRNA2. Cells were treated with the indicated doses of Mitomycin C and cell viability analyzed by the MTT assay. Data are displayed as percent cell viability relative to untreated cells. Error bars represent +/- SEM from three independent experiments performed in duplicate.

Supplemental Figure 5

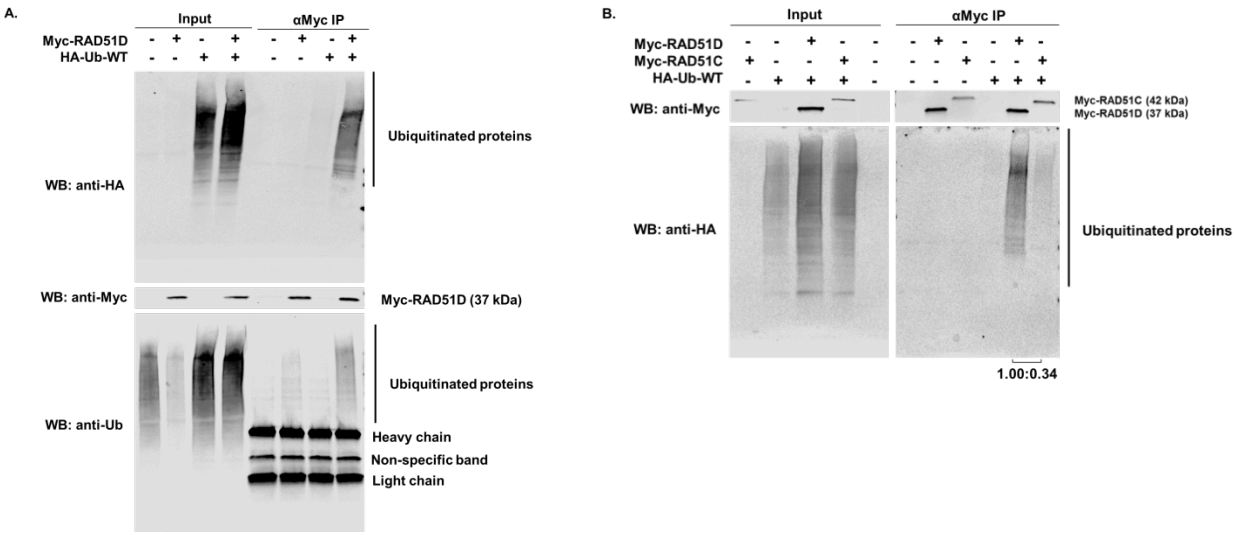

Fig. S5. RAD51D is ubiquitinated in the absence of over-expressed RNF138 and in the presence of MG132. (A). HeLa cells were individually transfected with Myc-RAD51D, HA-Ub-WT, or both and treated with 25 μM MG132. Three hundred micrograms of whole cell extract were added to anti-Myc magnetic beads. Whole cell extracts and IP samples were separated on a 4 – 20% acrylamide gradient gel. Anti-myc (rabbit polyclonal), anti-HA (rat monoclonal), or anti-Ub (mouse monoclonal) primary antibody was used. Note the lower protein concentration in lane 2 of the anti-Ub blot. Heavy and light chains from the beads used for immunoprecipitation were detected with the anti-mouse secondary antibody. (B). HeLa cells were individually transfected with Myc-RAD51D or Myc-RAD51C, with or without HA-Ub-WT, and treated with 25 μM MG132. Whole cell extract and IP samples were analyzed as previously described. Densitometry measurements were performed using LiCor Image Studio software (v4.0). The anti-HA signal was normalized to the anti-Myc signal for each corresponding sample. The ratio of anti-HA signal between Myc-RAD51D and Myc-RAD51C is shown.